PERGAMON

International Journal of Solids and Structures 38 (2001) 4147–4172

INTERNATIONAL JOURNAL OF SOLIDS and STRUCTURES

www.elsevier.com/locate/ijsolstr

Micromechanical prediction of ultimate strength of transversely isotropic fibrous composites

Zheng-ming Huang *

Department of Mechanics, Huazhong University of Science and Technology, Wuhan, Hubei 430074, People's Republic of China

Received 19 June 1998; in revised form 13 June 2000

Abstract

This paper addresses a micromechanics based strength theory to estimate the ultimate strength of unidirectionally fiber reinforced composites. The fibers used can be transversely isotropic in an elastic region but become isotropically hardening in a plastic one. The matrix material is considered as isotropically elastic–plastic. The stress state generated in each constituent material is explicitly expressed as a function of overall applied loads by making use of a bridging matrix that correlates the stress state in the fibers with that in the matrix. In this way, the composite strength is treated in terms of those of the constituent materials. Whenever one of the constituent materials attains its failure stress state, the corresponding overall applied stress is defined as the ultimate strength of the composite. This is because in most cases either the fiber fracture or the matrix breaking is the source that initiates the composite failure. The well-developed maximum normal stress theory of isotropic materials is applied to govern the constituent failure. One of the best advantages of the present theory is that the composite strength can be well estimated using minimum number of input data, which are the constituent properties and the fiber volume fraction only. Another advantage is that the failure mode and the stress level in each constituent material are automatically indicated when the composite fails. Such information is important for composite design. The present theory has been used to predict the off-axial strengths or strength envelop of a number of unidirectional composites. Good correlation between the predicted strengths and available experimental data has been found. Application to laminate strength analysis has been shown. The simulated strength envelope of an angle-plied laminate using original constituent properties agrees well with experimental data. Comparison of this strength theory with another well-known phenomenological theory, the Tsai–Wu theory, shows that the present theory is grossly much more accurate for the considered laminate, which indicates that understanding of the matrix inelastic deformation is critical for laminate strength analysis.

Keywords: Fibrous composite; Multidirectional laminate; Mechanical property; Micromechanical simulation; Inelastic deformation; Constitutive relationship; Failure mode; Ultimate strength; Strength formulae

* Present address: Polymer laboratory, Department of Mechanical Production and Engineering, National University of Singapore, 10 Kent Ridge Crescent, Singapore 119260, Singapore. Fax: +65-776-6925.

E-mail address: huangzm@email.com (Z.-m. Huang).

0020-7683/01/$ - see front matter
PII: S0020-7683(00)00268-7

1. Introduction

Strength is an important mechanical property that must be taken into account in composite designs. Various formalisms have been used to predict the failure behavior of continuous fiber reinforced composites. Several comprehensive surveys on the available composite strength theories exist in the literature (see e.g. Tsai and Wu, 1972; Rowlands, 1985; Nahas, 1986; Labossiere and Neal, 1987; Echaabi et al., 1996). Recently, Hinton and Soden (1998) and Soden et al. (1998a), sponsored by the UK Engineering and Physical Science Research Council, organized a "failure exercise" to compare predictive capabilities of a number of the most important strength theories in current usage. It has been recognized that most of these theories are developed phenomenologically, treating the composites as homogeneous and anisotropic materials. In general, extensive experiments including, possibly, biaxial tests, which may be difficult or expensive to conduct in some circumstances, are necessary to determine the strength coefficients involved in these theories whenever they are applied to any particular composite. Even with the same constituent materials, different composites having different fiber reinforcements still require repeated tests. Another drawback with these phenomenological theories is that they usually cannot predict the failure mode of a composite. Namely, they are unable to indicate which of the constituent phases initiates the failure of the composite, and to tell the stress level of each constituent when the composite fails. From a designer's point of view, the micromechanical failure mechanisms of the composite are important. The quantitative relationship of the overall failure of the composite with the respective strengths of the constituent materials and with their composition geometry is important for choosing an existing composite and for designing a new composite. An accurate micromechanical approach to the failure of the composites can also save cost in experimentation required by a macromechanical approach.

A number of attempts have been made to micromechanically investigate the strength behavior of the fiber reinforced composites (see e.g. Skudra, 1985; Beaumont and Schultz, 1990; Curtin, 1993; Pindera 1993; Subramanian et al., 1995; Christensen, 1997; Gundel and Wawner, 1997; Gotsis et al., 1998). However, significant limitations exist behind their development. For example, in the Chamis's model (Gotsis et al., 1998) which is the only micromechanics failure theory to have joined the Soden et al. (1998a) exercise, the composite longitudinal tensile strength is computed from fiber tensile strength and the fiber volume fraction. This treatment is correct in the case that the stiffness and strength of the fiber are significantly higher than those of the matrix (see Eq. (23a) of this paper), but becomes obviously wrong in a reverse case. Other limitations include pre-assumed failure/deformation modes (see e.g. Skudra, 1985; Curtin, 1993; Christensen, 1997; Gundel and Wawner, 1997). Although Aboudi (1988, 1989) was able to estimate the strength of unidirectional fiber composites based on his method of cells model in a rather general sense, his model is much complicated for application. In fact, Teply and Reddy (1990) have shown that the method of cells model can be reformulated and cast in the form of a finite element analysis by employing the Hellinger–Reissner variational principle. The user-unfriendly feature of this model is thus clearly seen.

In this paper, a general and easy-to-use micromechanical strength theory is developed to estimate the ultimate tensile strength of continuous fiber reinforced composites under an arbitrary load condition. The theory focuses on determining the internal stresses generated in the constituent fiber and matrix materials. The stress state in each constituent phase is explicitly related to the overall applied stress. In this way, the composite strength can be treated in terms of those of the constituent materials. The composite failure is considered to occur as long as any constituent material attains its failure stress state. This is because in most cases either the fiber fracture or the matrix breaking is the source which initiates the composite failure. The well-developed maximum normal stress criterion of isotropic materials is used to detect the failure of the constituent material. However, any other strength criterion for single-phase constituent materials is also applicable. The ultimate tensile strength of the composite is thus defined as the corresponding overall applied stress under which the composite fractures. Extensive comparisons have been made between the

predicted strengths of various unidirectional composites, using the present theory, and the experimental data. High correlation has been found, which suggests the potential of the present theory for engineering application. Application of this theory to the ultimate strength analysis of laminated composites has been shown. The predicted strength envelope of an angle-plied laminate subjected to combined biaxial load conditions agrees well with available experimental data. The present theory prediction, using original constituent properties, is also compared with that based on another well-known phenomenological theory, the Tsai–Wu theory. The present prediction shows obvious superiority for the composite under consideration.

2. Stress states in constituent materials

Let us consider a representative volume element (RVE) of a unidirectional (UD) fiber reinforced composite, as shown in Fig. 1. Because many materials posses an ability of undergoing significant plastic deformation before their failure, the constituent plasticity must be taken into account in order that a general strength theory is developed for the composite. For simplicity, suppose that the fibers used are transversely isotropic in an elastic region but become isotropic in a plastic one. Typical such fibers include glass, aramid, carbon, graphite, silicon carbide, and boron fibers, which can be well considered as linearly elastic until rupture. The matrix, however, is assumed to be isotropically elastic–plastic. In such case, the resulting unidirectional composite is generally considered as a transversely isotropic material, having three material principal axes same as those of the fibers. Thus, for the composite and fibers, a rectangular coordinate system (1, 2, 3) is always set up in such a way that the coordinate 1 is along the fiber axis (Fig. 1).

The constitutive equations of a constituent material (fiber or matrix) can be cast, in an incremental form, as

$$\{\mathrm{d}\varepsilon_i\} = [S_{ij}]\{\mathrm{d}\sigma_j\}, \tag{1}$$

where $\{\mathrm{d}\varepsilon_i\} = \{\mathrm{d}\varepsilon_1, \mathrm{d}\varepsilon_2, \mathrm{d}\varepsilon_3, \mathrm{d}\varepsilon_4, \mathrm{d}\varepsilon_5, \mathrm{d}\varepsilon_6\}^{\mathrm{T}} = \{\mathrm{d}\varepsilon_{11}, \mathrm{d}\varepsilon_{22}, \mathrm{d}\varepsilon_{33}, 2\mathrm{d}\varepsilon_{23}, 2\mathrm{d}\varepsilon_{13}, 2\mathrm{d}\varepsilon_{12}\}^{\mathrm{T}}$, $\{\mathrm{d}\sigma_i\} = \{\mathrm{d}\sigma_1, \mathrm{d}\sigma_2, \mathrm{d}\sigma_3, \mathrm{d}\sigma_4, \mathrm{d}\sigma_5, \mathrm{d}\sigma_6\}^{\mathrm{T}} = \{\mathrm{d}\sigma_{11}, \mathrm{d}\sigma_{22}, \mathrm{d}\sigma_{33}, \mathrm{d}\sigma_{23}, \mathrm{d}\sigma_{13}, \mathrm{d}\sigma_{12}\}^{\mathrm{T}}$, and $[S_{ij}]$ is the elastic–plastic compliance matrix of the material having the form that (see Appendix A).

$$[S_{ij}] = \begin{cases} [S_{ij}]^{\mathrm{e}} & \text{when } \tau_0 \leqslant \frac{\sqrt{2}}{3}\sigma_{\mathrm{Y}}, \\ [S_{ij}]^{\mathrm{e}} + [S_{ij}]^{\mathrm{p}} & \text{when } \tau_0 > \frac{\sqrt{2}}{3}\sigma_{\mathrm{Y}}, \end{cases} \tag{2}$$

$$\tau_0 = \left[\tfrac{1}{3}\sigma'_{ij}\sigma'_{ij}\right]^{1/2}, \tag{3}$$

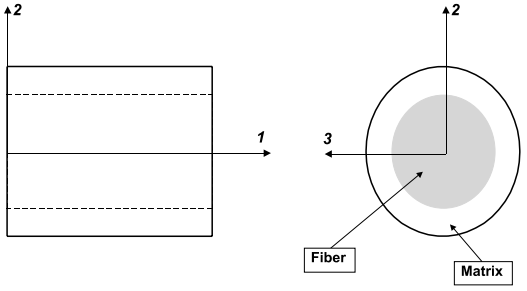

Fig. 1. An RVE of a UD composite.

$$\sigma'_{ij} = \sigma_{ij} - \tfrac{1}{3}\sigma_{kk}\delta_{ij}. \tag{4}$$

In Eqs. (3) and (4), a summation is applied to the repeated suffixes and σ_{ij} are total stresses. In Eq. (2), σ_Y is the yielding strength of the material under a uniaxial load and τ_0 is called an octahedral stress. $[S_{ij}]^e$ is the elastic component of the compliance matrix specified by the well known Hooke's law, i.e.,

$$[S_{ij}]^e = \begin{bmatrix} [S_{ij}]_\sigma & 0 \\ 0 & [S_{ij}]_\tau \end{bmatrix}, \tag{5a}$$

$$[S_{ij}]_\sigma = \begin{bmatrix} \frac{1}{E_{11}} & -\frac{v_{12}}{E_{11}} & -\frac{v_{12}}{E_{11}} \\ & \frac{1}{E_{22}} & -\frac{v_{23}}{E_{22}} \\ & \text{symmetric} & \frac{1}{E_{22}} \end{bmatrix}, \tag{5b}$$

$$[S_{ij}]_\tau = \begin{bmatrix} \frac{1}{G_{23}} & 0 & 0 \\ & \frac{1}{G_{12}} & 0 \\ & \text{symmetric} & \frac{1}{G_{12}} \end{bmatrix}, \tag{5c}$$

where E_{11} and E_{22} are Young's moduli in longitudinal and transverse directions of the materials, v_{12} and v_{23}, the Poisson ratios, and G_{12} and G_{23}, the shear moduli of the material, respectively. The moduli E_{22}, v_{23}, and G_{23} are not all independent but are related by

$$G_{23} = \frac{E_{22}}{2(1+v_{23})}. \tag{5d}$$

For an isotropic material, we have $E_{11} = E_{22} = E$, $v_{12} = v_{23} = v$, and $G_{12} = G_{23} = G = 0.5E/(1+v)$. $[S_{ij}]^p$ is the plastic component of the compliance matrix defined as (Appendix A)

$$[S_{ij}]^p = \frac{1}{2M_T\tau_0^2}\begin{bmatrix} \sigma'_{11}\sigma'_{11} & \sigma'_{22}\sigma'_{11} & \sigma'_{33}\sigma'_{11} & 2\sigma'_{23}\sigma'_{11} & 2\sigma'_{13}\sigma'_{11} & 2\sigma'_{12}\sigma'_{11} \\ & \sigma'_{22}\sigma'_{22} & \sigma'_{33}\sigma'_{22} & 2\sigma'_{23}\sigma'_{22} & 2\sigma'_{13}\sigma'_{22} & 2\sigma'_{12}\sigma'_{22} \\ & & \sigma'_{33}\sigma'_{33} & 2\sigma'_{23}\sigma'_{33} & 2\sigma'_{13}\sigma'_{33} & 2\sigma'_{12}\sigma'_{33} \\ & & & 4\sigma'_{23}\sigma'_{23} & 4\sigma'_{13}\sigma'_{23} & 4\sigma'_{12}\sigma'_{23} \\ & & & & 4\sigma'_{13}\sigma'_{13} & 4\sigma'_{12}\sigma'_{13} \\ & \text{symmetric} & & & & 4\sigma'_{12}\sigma'_{12} \end{bmatrix}, \tag{6a}$$

$$M_T = \frac{E_{11}E_T}{E_{11} - E_T}, \tag{6b}$$

where E_T is the hardening modulus (tangent to the stress–strain curve in plastic region) of the material under a uniaxial load. It should be noted that the plastic component (6a) can occur only under loading conditions. As long as there is an unloading, the compliance matrix of the material is simply given by the elastic component, $[S_{ij}]^e$. The total stress is updated through

$$[\sigma_{ij}] = [\sigma_{ij}] + [\mathrm{d}\sigma_{ij}]. \tag{7}$$

In the following, a quantity with suffix (superscript or subscript) f or m will indicate that it belongs to the fiber or matrix phase. For example, E^m and v^m will denote the Young's modulus and Poisson's ratio of the matrix, whereas E_T^m and σ_Y^m will represent the hardening modulus and yielding strength of the matrix, respectively. The corresponding quantity without any suffix will refer to the composite.

Suppose that a bridging matrix, $[A_{ij}]$, correlates the stress increment in the matrix with that in the fiber at any load level via

$$\{\mathrm{d}\sigma_i^{\mathrm{m}}\} = [A_{ij}]\{\mathrm{d}\sigma_j^{\mathrm{f}}\}. \tag{8}$$

Substituting Eq. (8) into the volume-averaged relations:

$$\{\mathrm{d}\sigma_i\} = V_{\mathrm{f}}\{\mathrm{d}\sigma_i^{\mathrm{f}}\} + V_{\mathrm{m}}\{\mathrm{d}\sigma_i^{\mathrm{m}}\}, \tag{9a}$$

$$\{\mathrm{d}\varepsilon_i\} = V_{\mathrm{f}}\{\mathrm{d}\varepsilon_i^{\mathrm{f}}\} + V_{\mathrm{m}}\{\mathrm{d}\varepsilon_i^{\mathrm{m}}\}, \tag{9b}$$

where V represents volume fraction, and making use of

$$\{\mathrm{d}\varepsilon_i^{\mathrm{f}}\} = [S_{ij}^{\mathrm{f}}]\{\mathrm{d}\sigma_j^{\mathrm{f}}\}, \tag{10a}$$

$$\{\mathrm{d}\varepsilon_i^{\mathrm{m}}\} = [S_{ij}^{\mathrm{m}}]\{\mathrm{d}\sigma_j^{\mathrm{m}}\}, \tag{10b}$$

$$\{\mathrm{d}\varepsilon_i\} = [S_{ij}]\{\mathrm{d}\sigma_j\} \tag{10c}$$

we obtain (with $[I]$ denoting a unit matrix)

$$\{\mathrm{d}\sigma_i^{\mathrm{f}}\} = (V_{\mathrm{f}}[I] + V_{\mathrm{m}}[A_{ij}])^{-1}\{\mathrm{d}\sigma_j\}, \tag{11}$$

$$\{\mathrm{d}\sigma_i^{\mathrm{m}}\} = [A_{ij}](V_{\mathrm{f}}[I] + V_{\mathrm{m}}[A_{ij}])^{-1}\{\mathrm{d}\sigma_j\}, \tag{12}$$

$$[S_{ij}] = (V_{\mathrm{f}}[S_{ij}^{\mathrm{f}}] + V_{\mathrm{m}}[S_{ij}^{\mathrm{m}}][A_{ij}])(V_{\mathrm{f}}[I] + V_{\mathrm{m}}[A_{ij}])^{-1}. \tag{13}$$

It is thus only necessary to specify the bridging matrix, $[A_{ij}]$. When both the fiber and the matrix undergo elastic deformation, the overall compliance matrix, given by Eq. (13), takes the form of Eqs. (5a)–(5c). Hence, there are only five independent elements involved in the bridging matrix. The general form of $[A_{ij}]$ is expressed as

$$[A_{ij}] = \begin{bmatrix} a_{11} & a_{12} & a_{13} & a_{14} & a_{15} & a_{16} \\ & a_{22} & a_{23} & a_{24} & a_{25} & a_{26} \\ & & a_{33} & a_{34} & a_{35} & a_{36} \\ & & & a_{44} & a_{45} & a_{46} \\ & & & & a_{55} & a_{56} \\ \text{zero} & & & & & a_{66} \end{bmatrix}. \tag{14}$$

Suppose that all the independent elements are arranged on the diagonal. The fifteen non-zero off-diagonal elements are to be solved by substituting Eq. (14) into Eq. (13) and making the resulting compliance matrix to be symmetric, i.e.,

$$S_{ji} = S_{ij}, \quad i,j = 1,2,\ldots,6. \tag{15}$$

The last element, which is a_{44}, is determined by using condition of Eq. (5d). Detailed discussions on the determination of the independent elements of the bridging matrix is omitted. We only give their formulae as follows:

$$a_{11} = E_{\mathrm{m}}/E_{\mathrm{f1}}, \tag{16a}$$

$$a_{22} = a_{33} = a_{44} = 0.5(1 + E_{\mathrm{m}}/E_{\mathrm{f2}}), \tag{16b}$$

$$a_{55} = a_{66} = 0.5(1 + G_{\mathrm{m}}/G_{\mathrm{f}}), \tag{16c}$$

where E_m, G_m, E_{f1}, E_{f2}, and G_f are called effective moduli and are defined as

$$E_m = \begin{cases} E^m & \text{when } \tau_0^m \leqslant \frac{\sqrt{2}}{3}\sigma_Y^m, \\ E_T^m & \text{when } \tau_0^m > \frac{\sqrt{2}}{3}\sigma_Y^m, \end{cases} \tag{17a}$$

$$G_m = \begin{cases} 0.5E^m/(1+\nu^m) & \text{when } \tau_0^m \leqslant \frac{\sqrt{2}}{3}\sigma_Y^m, \\ E_T^m/3 & \text{when } \tau_0^m > \frac{\sqrt{2}}{3}\sigma_Y^m, \end{cases} \tag{17b}$$

$$E_{f1} = \begin{cases} E_{11}^f & \text{when } \tau_0^f \leqslant \frac{\sqrt{2}}{3}\sigma_Y^f, \\ E_T^f & \text{when } \tau_0^f > \frac{\sqrt{2}}{3}\sigma_Y^f, \end{cases} \tag{17c}$$

$$E_{f2} = \begin{cases} E_{22}^f & \text{when } \tau_0^f \leqslant \frac{\sqrt{2}}{3}\sigma_Y^f, \\ E_T^f & \text{when } \tau_0^f > \frac{\sqrt{2}}{3}\sigma_Y^f, \end{cases} \tag{17d}$$

$$G_f = \begin{cases} G_{12}^f & \text{when } \tau_0^f \leqslant \frac{\sqrt{2}}{3}\sigma_Y^f, \\ E_T^f/3 & \text{when } \tau_0^f > \frac{\sqrt{2}}{3}\sigma_Y^f. \end{cases} \tag{17e}$$

Although detailed description is omitted, evidence to confirm the accuracy of formulae (16a)–(16c) is presented here. As long as the composites exhibit an elastic deformation, all the non-diagonal elements of Eq. (14) are found, from Eq. (15), to be zero except for a_{12} and a_{13} which are given by

$$a_{13} = a_{12} = (S_{12}^f - S_{12}^m)(a_{11} - a_{22})/(S_{11}^f - S_{11}^m). \tag{18}$$

By using Eqs. (16a)–(16c) and (18), the five effective engineering moduli of the composites are determined to be (to obtain E_{11} and ν_{12}, let $d\sigma_{11} \neq 0$ and all the other $d\sigma_{ij} = 0$; to derive E_{22}, let $d\sigma_{22} \neq 0$ or $d\sigma_{33} \neq 0$ and all the other $d\sigma_{ij} = 0$; etc.)

$$E_{11} = V_f E_{11}^f + V_m E^m, \tag{19a}$$

$$\nu_{12} = V_f \nu_{12}^f + V_m \nu^m, \tag{19b}$$

$$E_{22} = \frac{(V_f + V_m a_{11})(V_f + V_m a_{22})}{(V_f + V_m a_{11})(V_f S_{22}^f + a_{22} V_m S_{22}^m) + V_f V_m (S_{21}^m - S_{21}^f) a_{12}}, \tag{19c}$$

$$G_{12} = G^m \frac{(G_{12}^f + G^m) + V_f (G_{12}^f - G^m)}{(G_{12}^f + G^m) - V_f (G_{12}^f - G^m)}, \tag{19d}$$

$$G_{23} = \frac{0.5(V_f + V_m a_{22})}{V_f (S_{22}^f - S_{23}^f) + V_m a_{22} (S_{22}^m - S_{23}^m)}. \tag{19e}$$

It is seen that Eqs. (19a) and (19b), obtained based on Eq. (16a), are exactly the same as rule of mixture formulae, which are sufficiently accurate (McCullough, 1990). The Eq. (19d), obtained on by Eq. (16c), is an exact elastic solution for the in-plane shear modulus (Hyer, 1997). Only the accuracy of formula (16b), on which Eqs. (19c) and (19e) are derived, needs to be verified. This can be done by comparing predicted results of the present model with experiments and with another micromechanical model, the model by Chamis (1989). Fig. 2 shows comparison of predicted results using present and Chamis's models with experiments (Tsai and Hahn, 1980) for the transverse modulus of a glass/epoxy composite. A complete comparison of predicted various engineering moduli of the present model with measured results (Kriz and

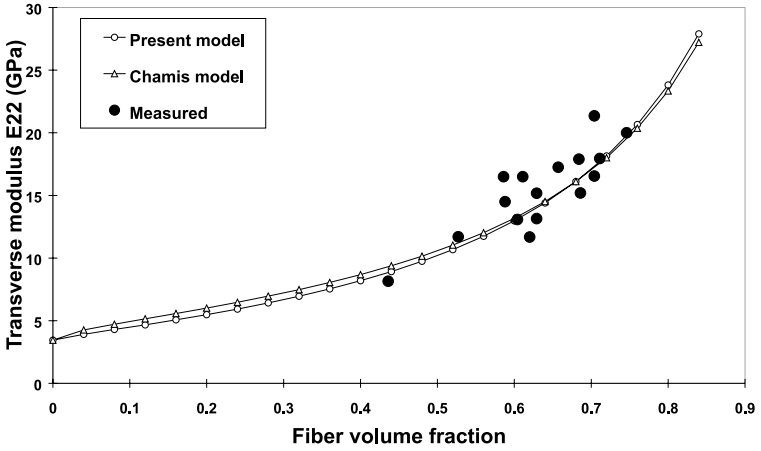

Fig. 2. Predicted and measured (Tsai and Hahn, 1982) transverse modulus of a glass/epoxy composite ($E_f = 73.1$ GPa, $E_m = 3.45$ GPa, $v_f = 0.22$, and $v_m = 0.35$).

Stinchcomb, 1979) of a carbon/epoxy composite varied with fiber volume fraction is indicated in Figs. 3–7. The material properties of the carbon fiber and epoxy matrix were taken from Aboudi (1984). High correlation in all these figures clearly indicates that formula (16b) as well as Eqs. (16a) and (16c) is sufficiently accurate in the elastic region.

Since the bridging matrix correlates the stresses generated in the two constituent materials of the composite, it can only depend on the material properties and on the packing geometries of the constituents. As long as the bridging matrix has been determined through an elastic deformation condition, only the material parameters involved need to be changed when any constituent material undergoes an inelastic deformation. This is because the packing geometries (such as the fiber volume fraction, the fiber arrangements in the matrix, and the fiber cross-sectional shape) do not change or only vary by negligibly

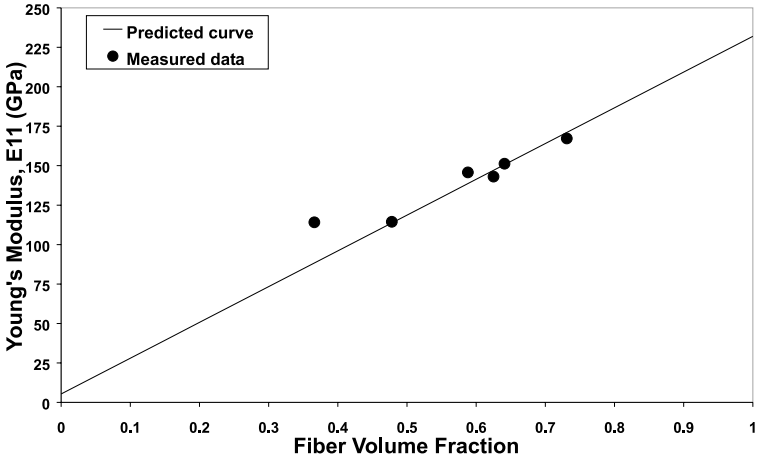

Fig. 3. Predicted and measured (Kriz and Stinchcomb, 1979) longitudinal modulus, E_{11}, of carbon/epoxy composites ($E_{11}^f = 232$ GPa, $v_{12}^f = 0.279$, $E_{22}^f = 15$ GPa, $v_{23}^f = 0.49$, $G_{12}^f = 24$ GPa, $E^m = 5.35$ GPa, and $v^m = 0.49$).

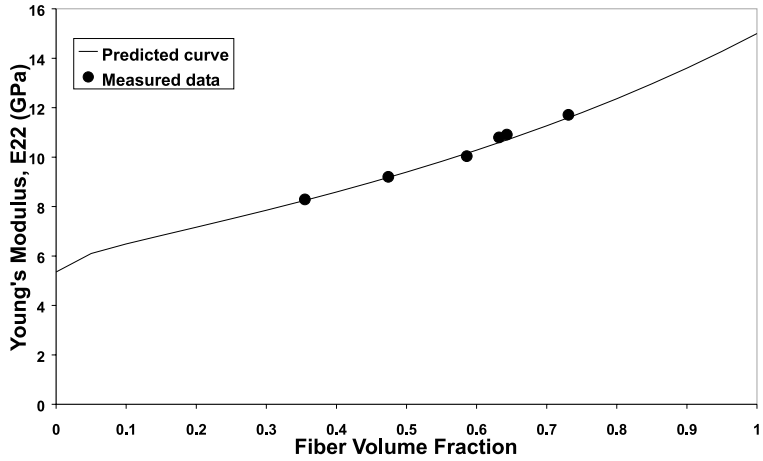

Fig. 4. Predicted and measured transverse modulus, E_{22}, of carbon/epoxy composites.

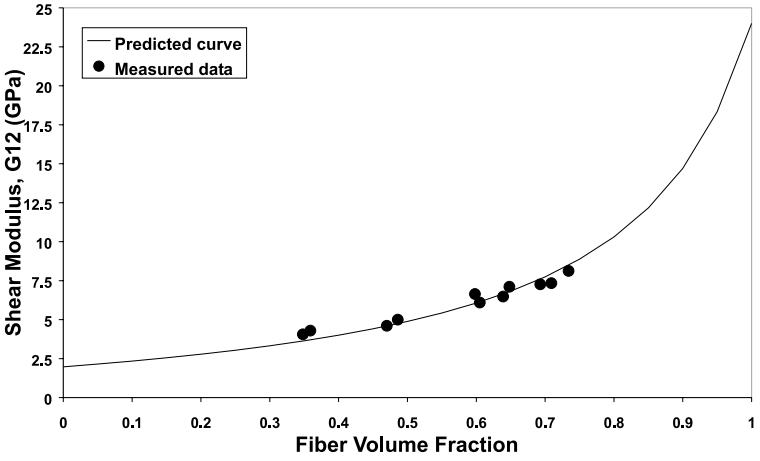

Fig. 5. Predicted and measured shear modulus, G_{12}, of carbon/epoxy composites.

small amount when the constituent undergoes the inelastic deformation. Therefore, formulae (16a)–(16c) are also applicable in a plastic region.

3. Strength theory

Eqs. (11) and (12) explicitly specify the stress increments generated in the fiber and matrix materials, respectively, due to the overall stress increment applied on the composite. Using Eq. (7), the total stresses in the fiber, matrix, and composite phases are all known at every load level. Based on these stresses, a strength theory for the composite can be developed in terms of those of the constituent materials. The theory postulates that except for two extreme cases in which the fiber volume fraction is either extremely small or extremely large, the composite is considered to fail whenever any of its constituent materials, either the fiber or the matrix, attains its ultimate stress. Here, the ultimate stress of a constituent material is understood to

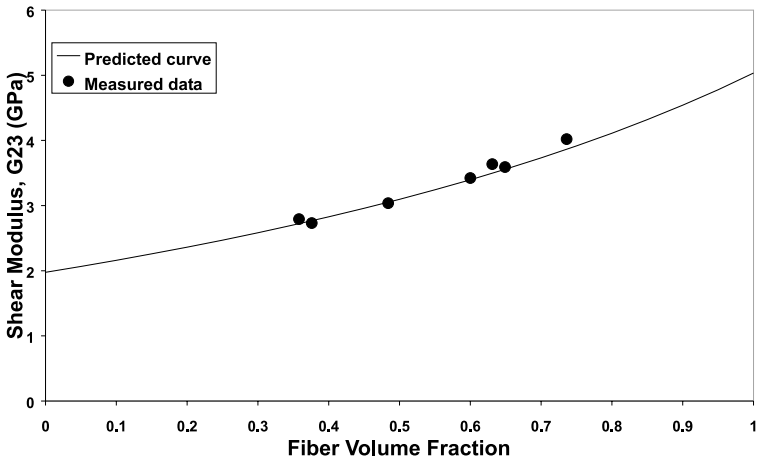

Fig. 6. Predicted and measured shear modulus, G_{23}, of carbon/epoxy composites.

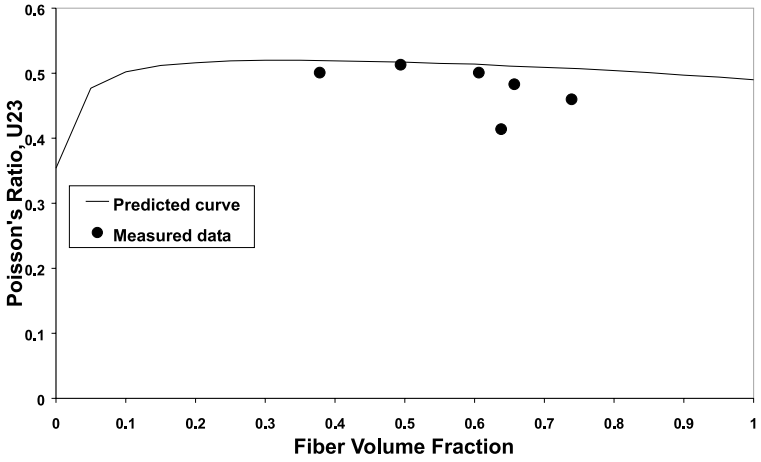

Fig. 7. Predicted and measured Poisson's ratio, v_{23}, of carbon/epoxy composites.

be the failure stress state according to some strength criterion that governs the failure of a single-phase homogeneous material. As we understand, there are essentially three sources, i.e., fiber fracture, matrix fracture, and fiber/matrix interface debonding, which cause the composite failure. Therefore, the postulation, on which the present theory will be developed, is reasonable as long as there is a perfect bonding along the interface between the fiber and the matrix. However, the interface debonding can also be apparently incorporated as though the matrix material (which is inferior in stiffness and strength relative to the fiber material) had a lower ultimate stress. Thus, only two failure modes, i.e., fiber breaking and matrix fracture, are concerned in the following.

For isotropic (matrix) materials, one of the most successful strength theories is the maximum normal stress criterion. It says that the material fails as soon as the maximum normal stress, σ^1, generated in the material reaches its ultimate value, no matter whether the material is under uniaxial or multiaxial state of stress. Here, σ^1 represents algebraically the largest one of the three principal stresses of the material, i.e.

$\sigma^1 \geqslant \sigma^2 \geqslant \sigma^3$. Supposing that the general stress state of the material is denoted by $(\sigma_{xx}, \sigma_{yy}, \sigma_{zz}, \sigma_{yz}, \sigma_{xz}, \sigma_{xy})$, the three principal stresses, σ^1, σ^2, and σ^3, are the solutions to the following eigenvalue equation:

$$\det\left(\begin{bmatrix} \sigma_{xx} & \sigma_{xy} & \sigma_{xz} \\ \sigma_{yx} & \sigma_{yy} & \sigma_{yz} \\ \sigma_{zx} & \sigma_{zy} & \sigma_{zz} \end{bmatrix} - \sigma[I]\right) = 0. \tag{20}$$

Hence, the failure criterion can be expressed as

$$\sigma^1 \geqslant \sigma_{\mathrm{u}}, \tag{21}$$

where σ_{u} is the ultimate tensile strength of the materials obtained from a uniaxial tension. Similarly, the material compressive failure is attained if

$$\sigma^3 \leqslant -\sigma_{\mathrm{u,c}}, \tag{22}$$

where $\sigma_{\mathrm{u,c}}$ is the ultimate compressive strength of the material under a uniaxial compression. It should be noted that no material buckling is involved herein.

On the other hand, there is no such failure criterion similar to Eq. (21), which is powerful and yet simple, for general single-phase transversely isotropic materials. Up to date, Tsai and Wu (1972) theory is considered to be one of the best phenomenological failure criteria for anisotropic (and hence transversely isotropic) materials (Christensen, 1997). However, a number of strength parameters including the ultimate stresses in longitudinal tension and compression, transverse tension and compression, biaxial and shear loads must be determined beforehand in order to apply this theory to the material. Most of these experiments are difficult to be carried out for the present fiber due to its small cross-sectional dimension. However, the small size (diameter) in the cross-sectional area of the fiber compared with its longitudinal dimension suggests that the fracture of the fiber is mainly caused by excessive load in the longitudinal direction. Considering that we aim at determining the ultimate tensile and compressive strengths of the composite, we can still use criteria (21) and (22) to check the failure status of the fiber even if it is transversely isotropic, where σ_{u} and $\sigma_{\mathrm{u,c}}$ should be understood to be the tensile and the compressive strengths along the fiber axial direction. When any of the constituents fail, the corresponding overall load is termed as the composite ultimate load and the composite strength is determined accordingly.

4. Tensile strength under uniaxial load

In general, explicit forms for the elastic–plastic stress states generated in the fiber and matrix under arbitrarily applied load condition may be difficult to obtain due to possible coupling between plastic normal and shear stresses (Eq. (6a)). If, however, the overall applied load is only unidirectional, coupling between the averaged normal and shear stresses will be negligible, and the explicit stress states in the constituents are able to be derived. Based on these explicit stresses, a simple formula for calculating the composite strength is obtainable, as explained below. For simplicity, suppose that the fiber material is linearly elastic until rupture and the matrix is bilinearly elastic–plastic.

Let us consider a longitudinal tensile load first. The stress balance in the RVE gives

$$\mathrm{d}\sigma_{11} = V_{\mathrm{f}}\mathrm{d}\sigma_{11}^{\mathrm{f}} + V_{\mathrm{m}}\mathrm{d}\sigma_{11}^{\mathrm{m}}.$$

Substituting Eq. (16a) into the previous equation, we obtain

$$\mathrm{d}\sigma_{11}^{\mathrm{f}} = \frac{\mathrm{d}\sigma_{11}}{V_{\mathrm{f}} + V_{\mathrm{m}}a_{11}} \quad \text{and} \quad \mathrm{d}\sigma_{11}^{\mathrm{m}} = \frac{a_{11}\mathrm{d}\sigma_{11}}{V_{\mathrm{f}} + V_{\mathrm{m}}a_{11}}.$$

Therefore, the longitudinal tensile strength of the composite due to longitudinal tensile load is simply given by

$$\sigma_{11}^{u} = \min\left\{ \frac{\sigma_u^f - (\alpha_{e1}^f - \alpha_{p1}^f)\sigma_{11}^0}{\alpha_{p1}^f}, \frac{\sigma_u^m - (\alpha_{e1}^m - \alpha_{p1}^m)\sigma_{11}^0}{\alpha_{p1}^m} \right\}, \tag{23a}$$

where

$$\sigma_{11}^0 = \min\left\{ \frac{\sigma_Y^m}{\alpha_{e1}^m}, \frac{\sigma_u^f}{\alpha_{e1}^f} \right\}, \tag{23b}$$

$$\alpha_{e1}^f = \frac{E_{11}^f}{V_f E_{11}^f + (1 - V_f)E^m}, \tag{23c}$$

$$\alpha_{e1}^m = \frac{E^m}{V_f E_{11}^f + (1 - V_f)E^m}, \tag{23d}$$

$$\alpha_{p1}^f = \frac{E_{11}^f}{V_f E_{11}^f + (1 - V_f)E_T^m}, \tag{23e}$$

$$\alpha_{p1}^m = \frac{E_T^m}{V_f E_{11}^f + (1 - V_f)E_T^m}. \tag{23f}$$

Similarly, if the composite is only subjected to a transverse tensile load, its ultimate transverse tensile strength is derived as

$$\sigma_{22}^{u} = \min\left\{ \frac{\sigma_u^f - (\alpha_{e2}^f - \alpha_{p2}^f)\sigma_{22}^0}{\alpha_{p2}^f}, \frac{\sigma_u^m - (\alpha_{e2}^m - \alpha_{p2}^m)\sigma_{22}^0}{\alpha_{p2}^m} \right\}, \tag{24a}$$

where

$$\sigma_{22}^0 = \min\left\{ \frac{\sigma_Y^m}{\alpha_{e2}^m}, \frac{\sigma_u^f}{\alpha_{e2}^f} \right\}, \tag{24b}$$

$$\alpha_{e2}^f = \frac{E_{22}^f}{V_f E_{22}^f + 0.5(1 - V_f)(E^m + E_{22}^f)}, \tag{24c}$$

$$\alpha_{e2}^m = \frac{0.5(E_{22}^f + E^m)}{V_f E_{22}^f + 0.5(1 - V_f)(E^m + E_{22}^f)}, \tag{24d}$$

$$\alpha_{p2}^f = \frac{E_{22}^f}{V_f E_{22}^f + 0.5(1 - V_f)(E_T^m + E_{22}^f)}, \tag{24e}$$

$$\alpha_{p2}^m = \frac{0.5(E_{22}^f + E_T^m)}{V_f E_{22}^f + 0.5(1 - V_f)(E_T^m + E_{22}^f)}. \tag{24f}$$

It should be pointed that although a transverse load also generates longitudinal stress components in both fiber and matrix, they are believed to be small compared with their transverse counterparts and have not been considered in Eq. (24a).

Further, the composite in-plane shear strength only due to an in-plane shear load (σ_{12}) reads

$$\sigma_{12}^{u} = \min\left\{ \frac{\sigma_u^f - (\alpha_{e3}^f - \alpha_{p3}^f)\sigma_{12}^0}{\alpha_{p3}^f}, \frac{\sigma_u^m - (\alpha_{e3}^m - \alpha_{p3}^m)\sigma_{12}^0}{\alpha_{p3}^m} \right\}, \tag{25a}$$

where

$$\sigma_{12}^0 = \min\left\{ \frac{\sigma_Y^m}{\sqrt{3}\alpha_{e3}^m}, \frac{\sigma_u^f}{\alpha_{e3}^f} \right\}, \tag{25b}$$

$$\alpha_{e3}^f = \frac{G_{12}^f}{V_f G_{12}^f + 0.5(1 - V_f)(G^m + G_{12}^f)}, \tag{25c}$$

$$\alpha_{e3}^m = \frac{0.5(G_{12}^f + G^m)}{V_f G_{12}^f + 0.5(1 - V_f)(G^m + G_{12}^f)}, \tag{25d}$$

$$\alpha_{p3}^f = \frac{3G_{12}^f}{3V_f G_{12}^f + 0.5(1 - V_f)(E_T^m + 3G_{12}^f)}, \tag{25e}$$

$$\alpha_{p3}^m = \frac{0.5(3G_{12}^f + E_T^m)}{3V_f G_{12}^f + 0.5(1 - V_f)(E_T^m + 3G_{12}^f)}. \tag{25f}$$

In Eqs. (25a) and (25b), the tensile strengths of the constituents have been used to govern their shear failure, according to Eq. (21). If the material parameters of the constituents under pure shear are employed, we obtain the composite shear strength as follows

$$\sigma_{12}^{u} = \min\left\{ \frac{\tau_u^f - (\alpha_{e3}^f - \alpha_{p4}^f)\tau^0}{\alpha_{p4}^f}, \frac{\tau_u^m - (\alpha_{e3}^m - \alpha_{p4}^m)\tau^0}{\alpha_{p4}^m} \right\}, \tag{26a}$$

where

$$\tau^0 = \min\left\{ \frac{\tau_Y^m}{\alpha_{e3}^m}, \frac{\tau_u^f}{\alpha_{e3}^f} \right\}, \tag{26b}$$

$$\alpha_{p4}^f = \frac{G_{12}^f}{V_f G_{12}^f + 0.5(1 - V_f)(G_T^m + G_{12}^f)}, \tag{26c}$$

$$\alpha_{p4}^m = \frac{0.5(G_T^m + G_{12}^f)}{V_f G_{12}^f + 0.5(1 - V_f)(G_T^m + G_{12}^f)}. \tag{26d}$$

τ_u^f is the fiber shear strength, τ_Y^m and τ_u^m are the yield and ultimate strengths of the matrix under pure shear load respectively. G_T^m is the hardening modulus of the matrix under pure shear.

5. Application to laminated composites

One of the most significant applications of the present theory is for analysing progressive failure process of laminated composites. It has been recognized that failure analysis and strength prediction of laminated composites has not been well addressed in the current literature (Hinton and Soden, 1998; Soden et al., 1998a). A main problem involved is that the load shared by each lamina in the laminate depends on the

instantaneous stiffness matrix of this as well as other laminae, which is not a constant up to the laminate failure in most cases. Whereas, a UD lamina is statically determinate under a failure test, it becomes always statically indeterminate in the laminate. Although a number of excellent lamina strength theories, such as Tsai and Wu (1972) and Hashin and Rotem (1973) theories, have been established, none of them can make a correct prediction if the load shared by the lamina is not determined accurately. However, the present theory automatically gives the lamina instantaneous compliance matrix (Eq. (13)), by incorporating the nonlinear deformation of any constituent material into account.

Suppose that the laminate under study consists of multidirectional laminae, stacking in different ply-angles. A global coordinate system (x, y, z), is assumed to have its origin on the middle surface of the laminate, with x and y in the laminate plane and z along the thickness direction. Let the fiber direction of the kth lamina to have an inclined ply-angle θ_k with the global x direction. Casting stress and strain in an incremental form, the classical laminated plate theory (Gibson, 1994) is applicable at any load level. Thus, only the in-plane stress and strain increments, i.e., $\{\mathrm{d}\sigma\}^G = \{\mathrm{d}\sigma_{xx}, \mathrm{d}\sigma_{yy}, \mathrm{d}\sigma_{xy}\}^{\mathrm{T}}$ and $\{\mathrm{d}\varepsilon\}^G = \{\mathrm{d}\varepsilon_{xx}, \mathrm{d}\varepsilon_{yy}, 2\mathrm{d}\varepsilon_{xy}\}^{\mathrm{T}}$, are retained, where G refers to the global coordinate system. The stresses increments sustained by the kth lamina in the laminate, $\{\mathrm{d}\sigma\}_k^G$, are related with the strain and curvature increments of the middle surface, i.e., $\mathrm{d}\varepsilon_{xx}^0$ etc. and $\mathrm{d}\kappa_{xx}^0$ etc., through (Gibson, 1994)

$$\{\mathrm{d}\sigma\}_k^G = [(C_{ij}^G)_k]\{\mathrm{d}\varepsilon\}_k^G = ([T]_{\mathrm{c}})_k([S]_k)^{-1}([T]_{\mathrm{c}}^{\mathrm{T}})_k\{\mathrm{d}\varepsilon\}_k^G, \tag{27}$$

where

$$\{\mathrm{d}\varepsilon\}_k^G = \left\{\mathrm{d}\varepsilon_{xx}^0 + \frac{z_k + z_{k-1}}{2}\mathrm{d}\kappa_{xx}^0, \mathrm{d}\varepsilon_{yy}^0 + \frac{z_k + z_{k-1}}{2}\mathrm{d}\kappa_{yy}^0, 2\mathrm{d}\varepsilon_{xy}^0 + (z_k + z_{k-1})\mathrm{d}\kappa_{xy}^0\right\}^{\mathrm{T}} \tag{28}$$

and z_k and z_{k-1} are the z coordinates of the top and bottom surfaces of the lamina. In Eq. (27), $[S]_{3\times3}$ is the planar compliance matrix of the lamina in its local coordinate system, adapted from Eq. (13), and $[T]_{\mathrm{c}}$ is a coordinate transformation matrix given by

$$[T]_{\mathrm{c}} = \begin{bmatrix} l_1^2 & l_2^2 & 2l_1l_2 \\ m_1^2 & m_2^2 & 2m_1m_2 \\ l_1m_1 & l_2m_2 & l_1m_2 + l_2m_1 \end{bmatrix}, \quad l_1 = m_2 = \cos\theta, \ \ l_2 = -m_1 = \sin\theta. \tag{29}$$

The middle surface strains and curvatures are obtained by considering laminate equilibrium condition, resulting in the following equations (Gibson, 1994):

$$\begin{Bmatrix} \mathrm{d}N_{xx} \\ \mathrm{d}N_{yy} \\ \mathrm{d}N_{xy} \\ \mathrm{d}M_{xx} \\ \mathrm{d}M_{yy} \\ \mathrm{d}M_{xy} \end{Bmatrix} = \begin{bmatrix} Q_{11}^{\mathrm{I}} & Q_{12}^{\mathrm{I}} & Q_{16}^{\mathrm{I}} & Q_{11}^{\mathrm{II}} & Q_{12}^{\mathrm{II}} & Q_{16}^{\mathrm{II}} \\ Q_{12}^{\mathrm{I}} & Q_{22}^{\mathrm{I}} & Q_{26}^{\mathrm{I}} & Q_{12}^{\mathrm{II}} & Q_{22}^{\mathrm{II}} & Q_{26}^{\mathrm{II}} \\ Q_{16}^{\mathrm{I}} & Q_{26}^{\mathrm{I}} & Q_{66}^{\mathrm{I}} & Q_{16}^{\mathrm{II}} & Q_{26}^{\mathrm{II}} & Q_{66}^{\mathrm{II}} \\ Q_{11}^{\mathrm{II}} & Q_{12}^{\mathrm{II}} & Q_{16}^{\mathrm{II}} & Q_{11}^{\mathrm{III}} & Q_{12}^{\mathrm{III}} & Q_{16}^{\mathrm{III}} \\ Q_{12}^{\mathrm{II}} & Q_{22}^{\mathrm{II}} & Q_{26}^{\mathrm{II}} & Q_{12}^{\mathrm{III}} & Q_{22}^{\mathrm{III}} & Q_{26}^{\mathrm{III}} \\ Q_{16}^{\mathrm{II}} & Q_{26}^{\mathrm{II}} & Q_{66}^{\mathrm{II}} & Q_{16}^{\mathrm{III}} & Q_{26}^{\mathrm{III}} & Q_{66}^{\mathrm{III}} \end{bmatrix} \begin{Bmatrix} \mathrm{d}\varepsilon_{xx}^0 \\ \mathrm{d}\varepsilon_{yy}^0 \\ 2\mathrm{d}\varepsilon_{xy}^0 \\ \mathrm{d}\kappa_{xx}^0 \\ \mathrm{d}\kappa_{yy}^0 \\ 2\mathrm{d}\kappa_{xy}^0 \end{Bmatrix}, \tag{30}$$

with

$$Q_{ij}^{\mathrm{I}} = \sum_{k=1}^{N}\left(C_{ij}^G\right)_k(z_k - z_{k-1}), \qquad Q_{ij}^{\mathrm{II}} = \frac{1}{2}\sum_{k=1}^{N}\left(C_{ij}^G\right)_k(z_k^2 - z_{k-1}^2), \qquad Q_{ij}^{\mathrm{III}} = \frac{1}{3}\sum_{k=1}^{N}\left(C_{ij}^G\right)_k(z_k^3 - z_{k-1}^3). \tag{31}$$

In Eq. (31), N is the total number of lamina plies, and $\left(C_{ij}^G\right)_k$ are the stiffness elements of the kth lamina in the global system defined in Eq. (27). In Eq. (30), $\mathrm{d}N_{xx}$, $\mathrm{d}N_{yy}$, $\mathrm{d}N_{xy}$, $\mathrm{d}M_{xx}$, $\mathrm{d}M_{yy}$, and $\mathrm{d}M_{xy}$ are the overall incremental in-plane forces and moments per unit length exerted on the laminate. Supposing that applied in-plane total stresses are $(\sigma_{xx}^0, \sigma_{yy}^0, \sigma_{xy}^0)$, these forces and moments are defined, respectively, as

$$\mathrm{d}N_{xx} = \int_{-h/2}^{h/2} (\mathrm{d}\sigma_{xx}^0)\mathrm{d}z, \qquad \mathrm{d}N_{yy} = \int_{-h/2}^{h/2} (\mathrm{d}\sigma_{yy}^0)\mathrm{d}z, \qquad \mathrm{d}N_{xy} = \int_{-h/2}^{h/2} (\mathrm{d}\sigma_{xy}^0)\mathrm{d}z, \tag{32a}$$

$$\mathrm{d}M_{xx} = \int_{-h/2}^{h/2} (\mathrm{d}\sigma_{xx}^0) z\,\mathrm{d}z, \qquad \mathrm{d}M_{yy} = \int_{-h/2}^{h/2} (\mathrm{d}\sigma_{yy}^0) z\,\mathrm{d}z, \qquad \mathrm{d}M_{xy} = \int_{-h/2}^{h/2} (\mathrm{d}\sigma_{xy}^0) z\,\mathrm{d}z, \tag{32b}$$

where $h = \sum_{k=1}^{N} (z_k - z_{k-1})$.

It is evident from Eq. (27) that each lamina ply in the laminate may carry a different load share, and some ply must have failed first before others. As soon as one ply has failed, the remaining stiffness of the laminate must be reduced. Various reduction strategies have been proposed in the literature (Soden et al., 1998a). In this paper, the simplest and a straightforward reduction, i.e., the total reduction, is employed. Suppose that the k_0th lamina has failed. Then, the middle surface strain and curvature increments at the next load step are still calculated from Eq. (30), but with different instantaneous stiffness elements, which are redefined by

$$Q_{ij}^{\mathrm{I}} = \sum_{\substack{k=1 \\ k\neq k_0}}^{N} \left(C_{ij}^G\right)_k (z_k - z_{k-1}), \qquad Q_{ij}^{\mathrm{II}} = \frac{1}{2} \sum_{\substack{k=1 \\ k\neq k_0}}^{N} \left(C_{ij}^G\right)_k (z_k^2 - z_{k-1}^2), \qquad Q_{ij}^{\mathrm{III}} = \frac{1}{3} \sum_{\substack{k=1 \\ k\neq k_0}}^{N} \left(C_{ij}^G\right)_k (z_k^3 - z_{k-1}^3). \tag{33}$$

6. Results and discussion

6.1. Unidirectional composite

In this sub-section, the strength theory developed above is applied to estimate the ultimate tensile strengths of five unidirectional fibrous composites under different load combinations. Experimental results of all these composites are available. Extensive comparisons between the predictions and the experiments are intended to show the efficiency of the present micromechanics based strength theory. Except for the first composite for which the constituent materials are both isotropic, the other four composites considered are made using transversely isotropic fiber and isotropic matrix materials. The last four examples also illustrate the applicability of criterion (21) to non-isotropic fiber materials.

In the first example, let us consider a unidirectional SiC fiber and titanium (Ti) matrix composite, which is used in advanced aerospace propulsion systems. Gundel and Wawner (1997) made an experimental and theoretical investigation for the longitudinal tensile strength of the SiC/Ti (SCS-6/Ti-1100) composites with varying fiber reinforcements. Recently, Foster et al. (1998) also studied the unidirectional tensile strength of this composite numerically as well as theoretically. According to Gundel and Wawner's (1997) report, the SiC-fiber used is an isotropically elastic material until rupture, having a Young's modulus of $E_{\mathrm{f}} = 400$ GPa and a Poisson's ratio of $\nu_{\mathrm{f}} = 0.25$. The measured ultimate tensile strength of the extracted fiber specimens, however, varied from 2520 to 4540 MPa. In the present study, a fiber ultimate strength of $\sigma_{\mathrm{u}}^{\mathrm{f}} = 3480$ MPa, which was measured using fiber samples extracted from a composite panel whose tensile stress–strain curve was plotted in Fig. 6 of Gundel and Wawner (1997), is used. In Gundel and Wawner's measurement, the Ti matrix exhibited a typical bilinear elastic–plastic behavior (see Fig. 2 of Gundel and Wawner (1997)), having properties: $E^{\mathrm{m}} = 110$ GPa, $E_{\mathrm{T}}^{\mathrm{m}} = 2.16$ GPa, $\sigma_{\mathrm{Y}}^{\mathrm{m}} = 850$ MPa, $\sigma_{\mathrm{u}}^{\mathrm{m}} = 1000$ MPa, and $\nu^{\mathrm{m}} = 0.33$. Based on these constituent properties, the unidirectional tensile strengths of the composites versus fiber volume fractions were easily calculated using Eq. (23a). For example, with $V_{\mathrm{f}} = 0.15$, the calculated composite tensile strength is 1246.2 MPa, which is in between measured values of 1150 and 1252 MPa (as a comparison, the Chamis's model (Gotsis et al., 1998 would give this strength as 522 MPa, which is much underestimated). The calculated strengths are plotted in Fig. 8. For comparison, the measured strengths

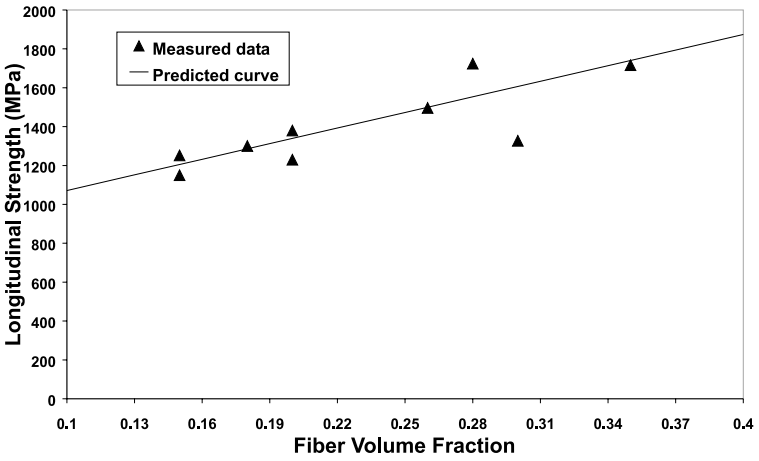

Fig. 8. Predicted and measured longitudinal tensile strength of composite versus fiber volume fraction. The material properties used are $E_f = 400$ GPa, $v_f = 0.25$, $\sigma_u^f = 3480$ MPa, $E^m = 110$ GPa, $E_T^m = 2.16$ GPa, $\sigma_Y^m = 850$ MPa, $\sigma_u^m = 1000$ MPa, and $v^m = 0.33$ (Gundel and Wawner, 1997).

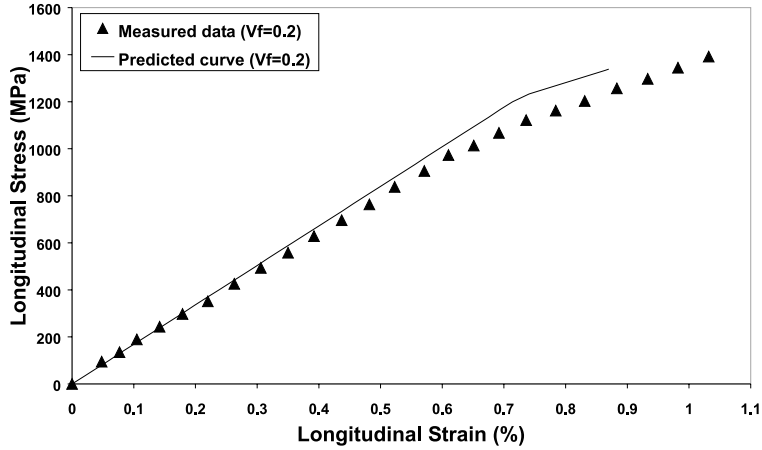

Fig. 9. Predicted and measured stress–strain curves of a composite with 20 percent fiber reinforcement, having same material properties as in Fig. 8.

taken from Table 5 of Gundel and Wawner (1997) are also given in the figure. Excellent correlation is seen to exist. In addition, predictions of the entire tensile stress–strain curves of two composites having 20% and 35% fiber reinforcements have also been made. These curves, together with the measured results taken from Gundel and Wawner (1997), are shown in Figs. 9 and 10, respectively. Good agreements between the predicted and measured curves have been found. In predicting the stress–strain curves, criterion (21) has been used to terminate a further calculation of the overall strain (using Eq. (10c)).

For the remaining composites, all the constituent material properties (elastic properties) are taken from Aboudi (1988, 1989). Let us consider the second example. It is a unidirectionally graphite fiber reinforced polyimide matrix composite, for which experiments were made by Pindera and Herakovich (1981). The material parameters used are (Aboudi, 1988): $E_{11}^f = 222$ GPa, $v_{12}^f = 0.33$, $E_{22}^f = 29.5$ GPa, $v_{23}^f = 0.73$,

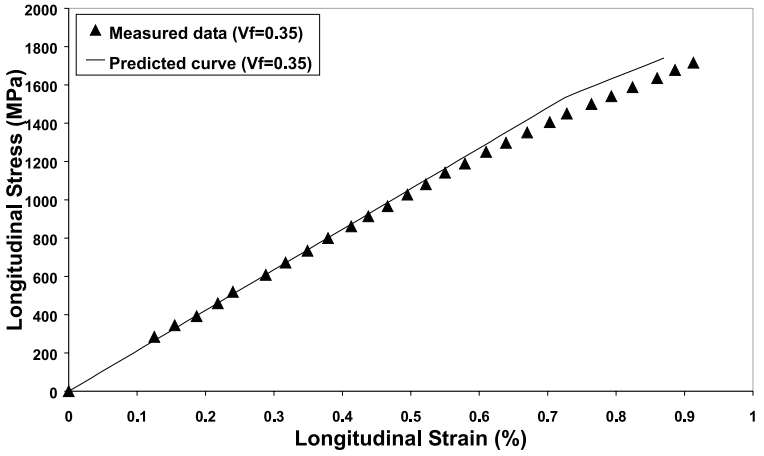

Fig. 10. Predicted and measured stress–strain curves of a composite with 35% fiber reinforcement, having same material properties as in Fig. 8.

$G_{12}^{f} = 24.1$ GPa, $E^{m} = 3.1$ GPa, and $v^{m} = 0.39$, with a fiber volume fraction of $V_f = 0.61$. In contrast to the first example, there are no available experimental data for the plastic and ultimate strength parameters of the graphite fiber and polyimide matrix materials. However, the overall longitudinal and transverse tensile strengths of the composite, $X = 1553.6$ MPa and $Y = 52$ MPa, were given in Pindera and Herakovich (1981), which can be used to retrieve these parameters.

The retrieving procedure is begun by assuming that the graphite fiber is linearly elastic until rupture. As the stiffness of the fiber is much higher than that of the matrix, we can imagine that the transverse tensile strength of the composite is governed by the strength of the matrix. Therefore, Eq. (24a) gives

$$\sigma_{22}^{u} = \frac{\sigma_{Y}^{m}}{\alpha_{e2}^{m}} + \frac{\sigma_{u}^{m} - \sigma_{Y}^{m}}{\alpha_{p2}^{m}} = Y \approx \frac{\sigma_{u}^{m}}{\alpha_{e2}^{m}}, \tag{34}$$

since $\alpha_{p2}^{m} \approx \alpha_{e2}^{m}$. From Eq. (34), the matrix strength is determined to be 34.8 MPa. Next, let us use Eq. (23a) to recover the fiber strength. It is required that

$$\sigma_{11}^{u} = \min\left\{ \frac{\sigma_{u}^{f} - (\alpha_{e1}^{f} - \alpha_{p1}^{f})\sigma_{11}^{0}}{\alpha_{p1}^{f}}, \frac{\sigma_{u}^{m} - (\alpha_{e1}^{m} - \alpha_{p1}^{m})\sigma_{11}^{0}}{\alpha_{p1}^{m}} \right\} = X.$$

At this stage, we cannot assume that $\alpha_{p1}^{m} \approx \alpha_{e1}^{m}$. However, the longitudinal strength of the composite is most probably governed by the strength of the fiber. Thus, we can consider $X = \sigma_{11}^{u} \approx \sigma_{u}^{f}/\alpha_{e1}^{f}$, due to $\alpha_{p1}^{f} \approx \alpha_{e1}^{f}$, providing that we can choose the other two parameters of the matrix, E_{T}^{m} and σ_{Y}^{m}, such that

$$\left(\frac{\sigma_{Y}^{m}}{\alpha_{e1}^{m}} + \frac{\sigma_{u}^{m} - \sigma_{Y}^{m}}{\alpha_{p1}^{m}} \right)_{\sigma_{u}^{m}=34.8\ \mathrm{MPa}} \geqslant X. \tag{35}$$

It is obvious that many different combinations of E_{T}^{m} and σ_{Y}^{m}, which satisfy inequality (35), exist. Hence, the recovered fiber strength is $\sigma_{u}^{f} = 2524.3$ MPa. Since $\left(\sigma_{u}^{m}/\alpha_{e1}^{m}\right)_{\sigma_{u}^{m}=34.8\ \mathrm{MPa}} < X$, the epoxy used cannot be considered as linearly elastic until rupture. On the other hand, any combination of E_{T}^{m} and σ_{Y}^{m}, which satisfies Eq. (35), is possible due to no other information available. For illustration, four different groups of E_{T}^{m} and σ_{Y}^{m} were used in the present calculation: the first was $E_{T}^{m} = 380$ MPa and $\sigma_{Y}^{m} = 20$ MPa, the second $E_{T}^{m} = 380$ MPa and $\sigma_{Y}^{m} = 28$ MPa, the third $E_{T}^{m} = 580$ MPa and $\sigma_{Y}^{m} = 20$ MPa, and the fourth $E_{T}^{m} = 580$ MPa and $\sigma_{Y}^{m} = 28$ MPa. These plastic parameters were chosen somewhat arbitrarily. However, the pre-

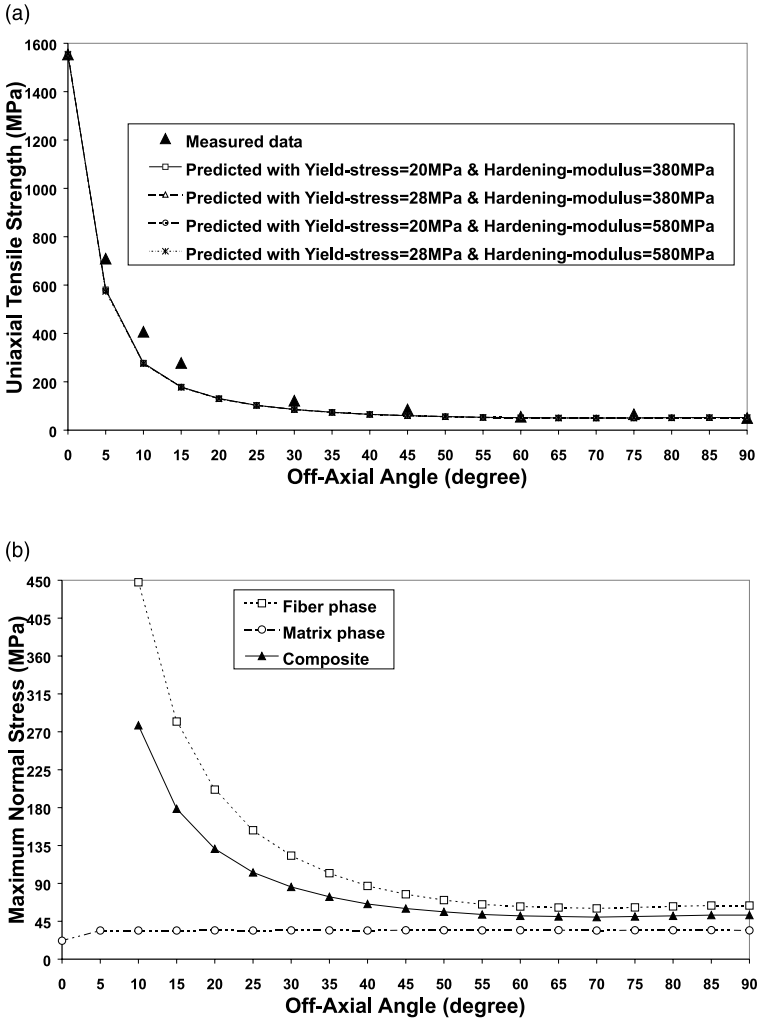

Fig. 11. (a) Predicted and measured off-axial strength of a unidirectional graphite/polyimide composite. The parameters used are $E_{11}^{f} = 222$ GPa, $v_{12}^{f} = 0.33$, $E_{22}^{f} = 29.5$ GPa, $v_{23}^{f} = 0.73$, $G_{12}^{f} = 24.1$ GPa, $\sigma_{u}^{f} = 2530$ MPa, $E^{m} = 3.1$ GPa, $v^{m} = 0.39$, $\sigma_{u}^{m} = 34.5$ MPa, and $V_f = 0.61$ (Pindera and Herakovich, 1981) and (b) maximum normal stresses in the composite, fiber, and matrix versus off-axial angle ($E_{T}^{m} = 380$ MPa and $\sigma_{Y}^{m} = 20$ MPa).

dicted off-axial tensile strengths of the composite with these four different groups of plastic parameters were nearly the same, as indicated in Fig. 11(a), where slight amendments have been made for the ultimate strengths of the fiber and matrix due to consideration of the matrix plasticity. This is attributed to the fact that the ultimate strength of the composite is mainly dependent on the ultimate stresses, but less on the yield stress or hardening modulus, of the constituent materials, especially when the stiffness of the fiber is considerably higher than that of the matrix (Eqs. (23a)–(23f) and (24a)–(24f)). Another fact is that the each load increment on the UD composite has already been given explicitly. On the other hand, the composite strain depends on the overall compliance matrix which is dominated by the more ductile material properties. Hence, the ultimate strain and the entire stress–strain curve of the composite are dependent on the plastic parameters of the constituents. It is further induced that the laminate strength will depend heavily on

the constituent plastic deformation, because the load sustained by each lamina in the laminate depends on the lamina current strains.

For comparison, the experimental data taken from Pindera and Herakovich (1981) are also shown in Fig. 11(a). Correlation between the predicted results and the experimental data is high. Since the composite tensile strength is estimated from the ultimate stress of either the fiber or the matrix, the failure mode is automatically indicated. Fig. 11(b) shows the maximum normal stresses in the composite, fiber, and the matrix varied with off-axial angles, when the composite attains the corresponding tensile strength. The figure clearly indicates that except for a small neighborhood of angle $= 0°$, the composite failure (tensile strength) in any other direction is caused by the matrix fracture. The figure also indicates that the ultimate tensile strength of the composite in any direction is always higher than that of the matrix due to fiber reinforcement. It is noted that the tensile strength of the neat (unreinforced) polyimide matrix material is originally reported to be 37 MPa (Pindera and Herakovich, 1981), which is in close to 34.5 MPa, recovered from the overall transverse strength of the composite. This can be considered as a further confirmation of the accuracy of the present strength theory.

The next two composites considered are made from graphite (AS) fiber and epoxy (3501) matrix with a 66% fiber reinforcement, and from Aramid (Kevlar-49) fiber and epoxy matrix having a 0.55 fiber volume fraction, respectively. The elastic properties of the constituent materials used in these two composites, taken from Aboudi (1988), are summarized in Tables 1 and 2. No other material parameters except for the off-axial tensile strengths of the composites are available. As in the second example, the overall longitudinal and transverse tensile strengths (X and Y) of the composites, which are also listed in Tables 1 and 2, are used to determine the ultimate strengths of the constituent materials. Again, the matrix materials used in both the composites must be considered as elastic–plastic. The recovered material parameters are summarized in Tables 1 and 2, respectively. Using the constituent material parameters given in Tables and the corresponding fiber volume fractions ($V_f = 0.66$ and $V_f = 0.55$), the off-axial tensile strengths of the two composites varied with off-axial angles were predicted and are indicated in Figs. 12(a) and 13(a), respectively. The experimentally measured strength data, taken from Kriz and Stinchcomb (1979) for AS/3501 and from Pindera et al. (1986) for Aramid/epoxy composites, are also shown in the figures. Satisfactory agreements are seen to exist between the theoretical and experimental results. Figs. 12(b) and 13(b) indicate the corresponding maximum normal stresses generated in the fibers and matrices when the off-axial tensile stresses of the composites attain their ultimate values. The quantitative behaviors of these two figures are similar to that of Fig. 11(b).

The last UD composite example considered is also made from graphite fibers and an epoxy matrix. The constituent materials of the composite have elastic properties (Aboudi, 1989): $E_{11}^f = 213.7$ GPa, $v_{12}^f = 0.2$, $E_{22}^f = 13.8$ GPa, $v_{23}^f = 0.25$, $G_{12}^f = 13.8$ GPa, $E^m = 3.45$ GPa, and $v^m = 0.35$, with a fiber volume fraction of $V_f = 0.66$. In contrast to the previous examples where only uniaxial loads were applied, the present com-

Table 1
Material parameters of AS graphite fibers and 3501 epoxy matrix UD composite ($X = 1500$ MPa, $Y = 51.7$ MPa and $V_f = 0.66$)

	E_{11} (GPa)	E_{22} (GPa)	v_{12}	v_{23}	G_{12} (GPa)	E_T (MPa)	σ_Y (MPa)	σ_u (MPa)
Graphite	213.7	13.8	0.2	0.25	13.8			2260
Epoxy	3.45	3.45	0.35	0.35	1.3	380	20	35

Table 2
Material parameters of Aramid fibers and an epoxy matrix UD composite ($X = 1141$ MPa, $Y = 27.3$ MPa and $V_f = 0.55$)

	E_{11} (GPa)	E_{22} (GPa)	v_{12}	v_{23}	G_{12} (GPa)	E_T (MPa)	σ_Y (MPa)	σ_u (MPa)
Aramid	124.1	4.1	0.35	0.35	2.9			2060
Epoxy	3.45	3.45	0.35	0.35	1.3	280	16	24

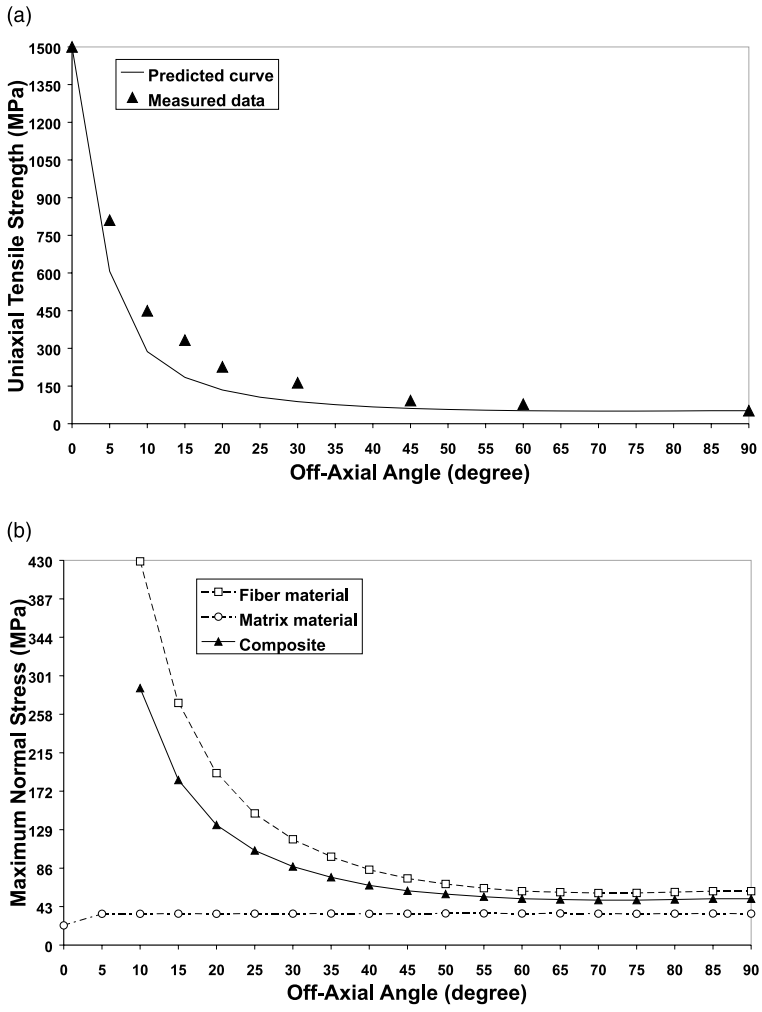

Fig. 12. (a) Predicted and measured off-axial strength of a unidirectional graphite/epoxy composite. The parameters used are $E_{11}^{f} = 213.7$ GPa, $v_{12}^{f} = 0.2$, $E_{22}^{f} = 13.8$ GPa, $v_{23}^{f} = 0.25$, $G_{12}^{f} = 13.8$ GPa, $\sigma_{u}^{f} = 2260$ MPa, $E^{m} = 3.45$ GPa, $v^{m} = 0.35$, $E_{T}^{m} = 380$ MPa, $\sigma_{Y}^{m} = 20$ MPa, $\sigma_{u}^{m} = 35$ MPa, and $V_{f} = 0.66$ (Kriz and Stinchcomb, 1979) and (b) maximum normal stresses in the composite, fiber, and matrix versus off-axial angle.

posite is under combined transverse tensile and axial shear loads (i.e., σ_{22} and σ_{12}). The failure envelope of this composite versus different combinations of σ_{22} and σ_{12} was experimentally measured by Awerbuch and Hahn (1981). The transverse tensile and in-plane shear strengths of the composite were (Awerbuch and Hahn, 1981): $Y = 60$ MPa (when $\sigma_{12} = 0$) and $S = 86.35$ MPa (when $\sigma_{22} = 0$), respectively. Based on these data, we can calculate back the ultimate strengths of the constituent materials. From the previous examples (examples 2 and 3), it can be expected that these stress levels may hardly cause the failure of the graphite fibers (as the stiffness and strength of the graphite fibers are much higher than those of the epoxy matrix, the fiber fracture would be mainly caused by excessive load in the longitudinal direction). Hence, the composite failures should be resulted from the matrix fracture. Using the given transverse tensile strength, $Y = 60$ MPa, the recovered matrix strength is 43 MPa, no matter whether the matrix is assumed to be linearly elastic or elastic–plastic. With this matrix strength, the predicted failure envelope of the composite is shown

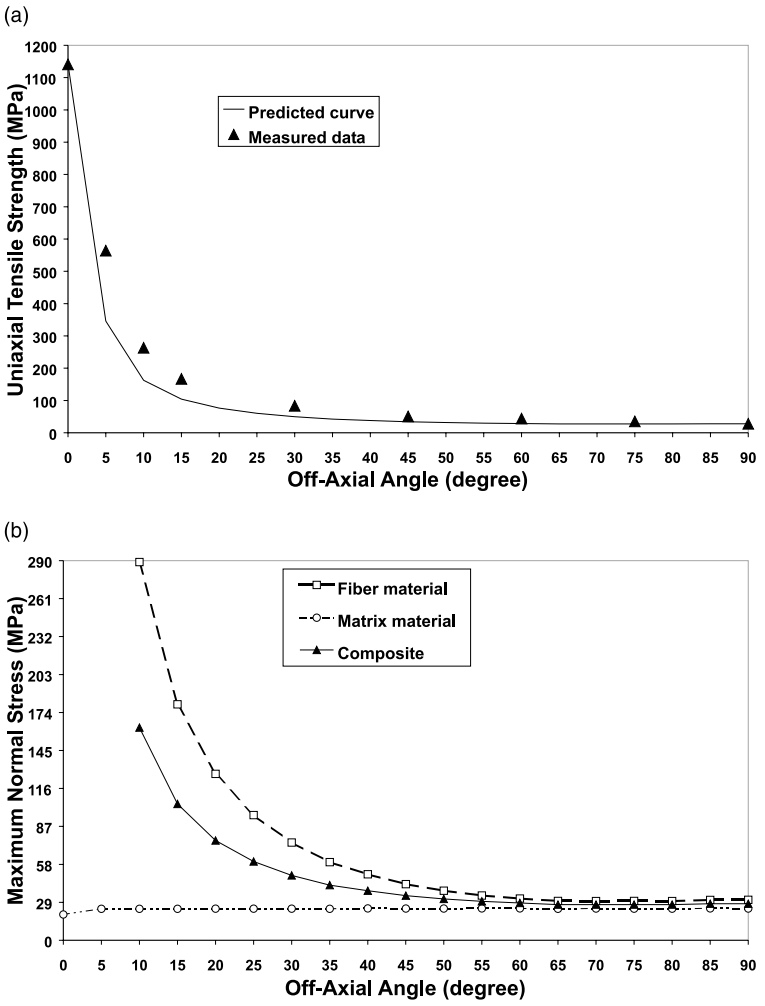

Fig. 13. (a) Predicted and measured off-axial strength of a unidirectional Aramid/epoxy composite. The parameters used are $E_{11}^{f} = 124.1$ GPa, $v_{12}^{f} = 0.35$, $E_{22}^{f} = 4.1$ GPa, $v_{23}^{f} = 0.35$, $G_{12}^{f} = 2.9$ GPa, $\sigma_{u}^{f} = 2060$ MPa, $E^{m} = 3.45$ GPa, $v^{m} = 0.35$, $E_{T}^{m} = 280$ MPa, $\sigma_{Y}^{m} = 16$ MPa, $\sigma_{u}^{m} = 24$ MPa, and $V_f = 0.55$ (Pindera et al., 1986) and (b) maximum normal stresses in the composite, fiber, and matrix versus off-axial angle.

in Fig. 14(a) by the broken-line. It can be seen from the figure that except for $\sigma_{12} = 0$, the predicted strength of the composite under every other combination of σ_{22} and σ_{12} is lower than a measured datum. Therefore, the graphite fibers cannot fail first before the matrix fractures under all the considered load combinations. More evidence can be gained from the resulting maximum normal stresses in the fiber and matrix, which are plotted in Fig. 14(b). These stresses are generated when the composite is loaded to the failure envelope, which is controlled by the matrix strength of 43 MPa, and are plotted versus the in situ transverse tensile stress. On the other hand, the recovered ultimate strength of the matrix is 54.5 MPa if the overall shear strength of the composite, $S = 86.35$ MPa, is used. Based on this matrix strength, the predicted failure envelope, as shown by the solid line in Fig. 14(a), agrees even better with the measured data for all the considered load combinations except for $\sigma_{12} = 0$. It seems that the predicted curve based on $\sigma_{u}^{m} = 54.5$ MPa should be more realistic. The corresponding maximum normal stresses generated in the fiber and matrix

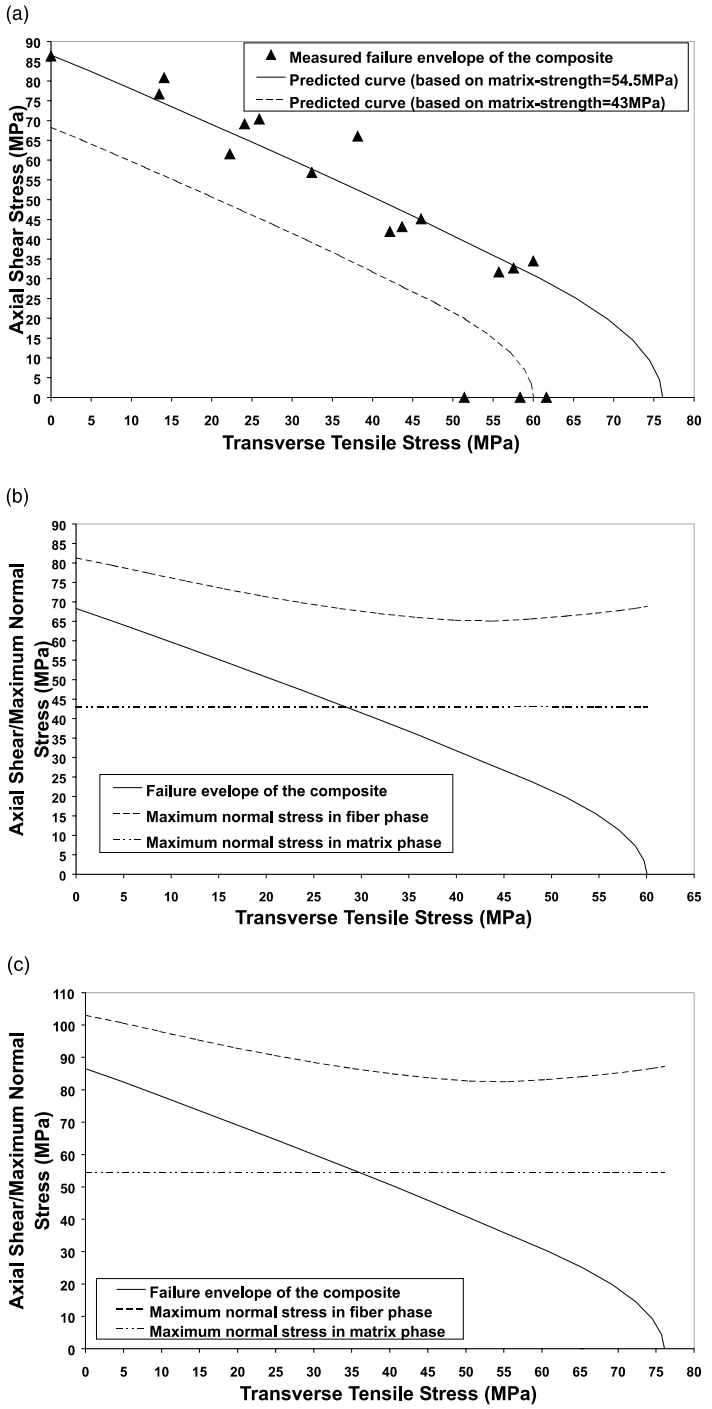

Fig. 14. (a) Predicted and measured failure envelope of a unidirectional graphite/epoxy composite. The parameters used are $E_{11}^{f} = 213.7$ GPa, $v_{12}^{f} = 0.2$, $E_{22}^{f} = 13.8$ GPa, $v_{23}^{f} = 0.25$, $G_{12}^{f} = 13.8$ GPa, $E^{m} = 3.45$ GPa, $v^{m} = 0.35$, and $V_{f} = 0.66$ (Awerbuch and Hahn, 1981), (b) maximum normal stresses in fiber and matrix when the composite is loaded to failure envelope (predicted using $\sigma_{u}^{m} = 43$ MPa) and (c) maximum normal stresses in fiber and matrix when the composite is loaded to failure envelope (predicted using $\sigma_{u}^{m} = 54.5$ MPa).

phases are indicated in Fig. 14(c), which has similar legend meaning as Fig. 14(b). From Fig. 14(c), we can see that the maximum normal stress generated in the fiber under every combined transverse tensile and in-plane shear loads is below 110 MPa, much lower than an expected graphite fiber strength. Hence, all the failures of the composite must be resulted from the matrix fracture, as indicated by the dot-and-dash line in Fig. 14(c).

6.2. Laminated composite

Soden et al. (1993) measured the final failure envelope of a composite shell made from E-glass/epoxy $[\pm 55°]_s$ angle-plied laminate subjected to bi-axial tensions, i.e., tensile loads in axial (x-) and circumferential (y-) directions. Different bi-axial tensions were achieved through adjusting internal pressure and axial load. The E-glass fiber reinforcement was Silenka 051L, 1200 tex, and the epoxy resin system was Ciba–Geigy MY750/HY917/DY063. Properties of these constituent materials have been reported in Soden et al. (1998b). They are $E_f = 74$ GPa, $v_f = 0.22$, $\sigma_u^f = 2150$ MPa, $\sigma_{u,c}^f = 1450$ MPa, $E^m = 3.35$ GPa, $v^m = 0.35$, $\sigma_u^m = 80$ MPa, $\sigma_{u,c}^m = 120$ MPa, and $\varepsilon_u^m = 5\%$, where ε_u^m is the ultimate strain of the matrix. Therefore, the matrix used must have displayed an inelastic deformation before failure. On the other hand, no information was given for the matrix plastic parameters in Soden et al. (1998b). In the present analysis, a bilinear elastic–plastic behavior is assumed for the matrix. Taking a typical yield strength of $\sigma_Y^m = 50$ MPa, the matrix hardening modulus is found to be $E_T^m = 850$ MPa. Using these independent parameters, the predicted failure envelope of the laminate is plotted in Fig. 15. The experimental data by Soden et al. (1993) are also shown in the figure. It is seen that correlation between the predictions and the experiments is fairly good.

To understand better the efficiency of the present theory especially the role of material nonlinearity in the laminate strength analysis, prediction for the failure envelope of the laminate using another popular theory, the Tsai and Wu (1972) theory, has also been made, and are plotted in Fig. 15 for comparison. The uni-directional lamina strengths, which were used to determine the strength parameters involved in the Tsai–Wu theory, had been taken from Soden et al. (1998b). They are, respectively, the longitudinal tensile and compressive strengths $X = 1280$ MPa and $X' = 800$ MPa, the transverse tensile and compressive strengths

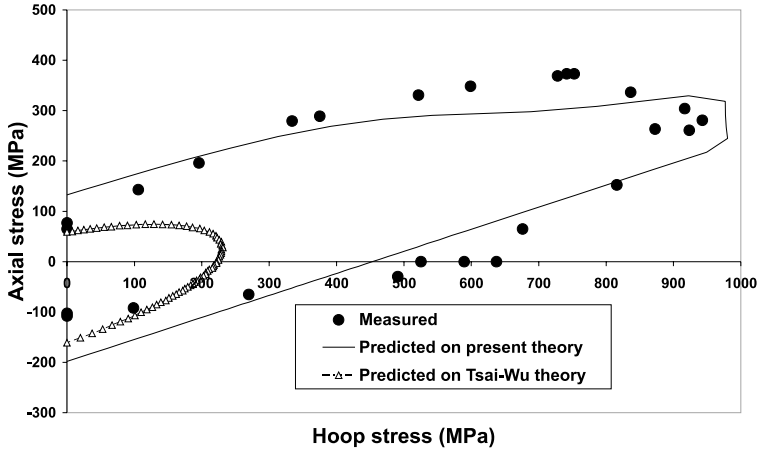

Fig. 15. Predicted and measured failure envelopes of a ±55° helical glass/epoxy shell subjected to combined axial and circumferential tensile loads. The parameters used are $E_f = 74$ GPa, $v_f = 0.22$, $\sigma_u^f = 2150$ MPa, $\sigma_{u,c}^f = 1450$ MPa, $E^m = 3.35$ GPa, $v^m = 0.35$, $\sigma_Y^m = 50$ MPa, $E_T^m = 850$ MPa, $\sigma_u^m = 80$ MPa, $\sigma_{u,c}^m = 120$ MPa, $V_f = 0.602$, $E_{11} = 45.6$ GPa, $E_{22} = 16.2$ GPa, $v_{12} = 0.278$, $G_{12} = 5.83$ GPa, $X = 1280$ MPa, $X' = 800$ MPa, $Y = 40$ MPa, $Y' = 145$ MPa, and $S = 73$ MPa (Soden et al., 1993, 1998b).

$Y = 40$ MPa and $Y' = 145$ MPa, and in-plane shear strength $S = 73$ MPa. In the prediction by using the Tsai–Wu theory, the lamina in-plane elastic properties, $E_{11} = 45.6$ GPa, $E_{22} = 16.2$ GPa, $v_{12} = 0.278$, $G_{12} = 5.83$ GPa, were also taken from Soden et al. (1998b), and, as usual, no matrix plasticity was assumed. It can be seen that the predicted failure envelope based on the present theory agree grossly much better with the experiments than that based on the Tsai–Wu theory. More applications as to all those "failure exercise" problems (Soden et al., 1998a) are reported elsewhere (Huang, 2000).

7. Conclusion

A powerful and user-friendly micromechanics based strength theory is described in this paper to predict the ultimate strength of transversely isotropic fiber reinforced isotropic matrix composites under any load condition. The biggest difference of the present theory, relative to those existing micromechnics models, is that the constituent nonlinear deformation has been taken into account reasonably. This nonlinearity is important for laminate failure analysis and strength prediction. The theory is developed based on a perfect bonding assumption for the fiber/matrix interface. There is no other limitation on the fiber and matrix materials used, except that the constitutive relationships of these materials can be described by Hooke's law, in their elastic region, and by the Prandtl–Reuss theory, in the plastic one, respectively. Extensive comparisons have been made between the predicted strengths of this theory and the available measured data. Good agreements exist in all the cases. In contrast to a macromechanical (phenomenological) strength theory, the present theory can clearly indicate the failure mode of the composites and the stress level in each constituent material when the composites fail. This makes it possible to optimize a composite strength by choosing proper constituent materials as well as fiber reinforcement/laminate lay-ups. Another advantage of the present theory is that it only uses a minimum number of experimental data from the constituents and no repeated test is required. Further improvement of the present theory could be made by discounting explicitly those geometric/fabrication defects such as damage evolution, fiber/matrix debonding, constituent buckling, etc. in the bridging matrix. Another improvement might also be possible by using different strength criterion to detect the constituent failure. For example, it is known that the maximum normal stress criterion is not very accurate in some load conditions such as pure shear, equi-multiaxial tensions, etc. Incorporation of the present micromechanics theory with a phenomenological failure criterion such as Tsai–Wu theory for laminate strength prediction is also possible.

Appendix A

In order to tailor the elastic–plastic behavior of a constituent material, a plastic flow theory must be applied. In this paper, we choose to use the general Prandtl–Reuss theory (Adams, 1974) to describe the isotropic hardening of the material. Using an incremental form, this flow theory postulates that the plastic incremental strain is proportional to the deviatoric stress, i.e.,

$$\mathrm{d}\varepsilon_{ij}^{(\mathrm{p})} = \mathrm{d}\lambda\sigma'_{ij}, \tag{A.1}$$

$$\sigma'_{ij} = \sigma_{ij} - \tfrac{1}{3}\sigma_{kk}\delta_{ij}, \tag{A.2}$$

where $\mathrm{d}\varepsilon_{ij}^{(\mathrm{p})}$ denote the strain increments in a plastic region, $\mathrm{d}\lambda$ is a positive parameter. The parameter $\mathrm{d}\lambda$ can be defined simply by multiplying Eq. (A.1) by itself. This gives

$$\mathrm{d}\lambda = \left[\mathrm{d}\varepsilon_{ij}^{(\mathrm{p})}\mathrm{d}\varepsilon_{ij}^{(\mathrm{p})}\right]^{1/2} \Big/ \left(\sigma'_{ij}\sigma'_{ij}\right)^{1/2}. \tag{A.3}$$

The total strain increments can be separated into

$$d\varepsilon_{ij} = d\varepsilon_{ij}^{(e)} + d\varepsilon_{ij}^{(p)}, \tag{A.4}$$

where the elastic components are related to the stress increments through Hooke's law, i.e.,

$$\{d\varepsilon_i^{(e)}\} = [S_{ij}]^{(e)}\{d\sigma_j\}. \tag{A.5}$$

Defining the octahedral plastic shear strain increment as

$$d\varepsilon_0^{(p)} = \left[\tfrac{1}{3}d\varepsilon_{ij}^{(p)}d\varepsilon_{ij}^{(p)}\right]^{1/2}, \tag{A.6}$$

and the octahedral shear stress as

$$\tau_0 = \left[\tfrac{1}{3}\sigma'_{ij}\sigma'_{ij}\right]^{1/2}, \tag{A.7}$$

Eq. (A.3) becomes

$$d\lambda = d\varepsilon_0^{(p)}/\tau_0. \tag{A.8}$$

Substituting the last equation into Eq. (A.1), we have

$$d\varepsilon_{ij}^{(p)} = \left(\frac{d\varepsilon_0^{(p)}}{\tau_0}\right)\sigma'_{ij}. \tag{A.9}$$

In order to establish a relationship between $d\varepsilon_0^{(p)}$ and τ_0, let us apply Eq. (A.9) to a uniaxial tensile test in which

$$\sigma_{22} = \sigma_{33} = \sigma_{12} = \sigma_{13} = \sigma_{23} = 0, \qquad \sigma_{11} \neq 0, \tag{A.10}$$

$$d\varepsilon_{12}^{(p)} = d\varepsilon_{23}^{(p)} = d\varepsilon_{13}^{(p)} = 0, \qquad d\varepsilon_{22}^{(p)} = d\varepsilon_{33}^{(p)} = -\tfrac{1}{2}d\varepsilon_{11}^{(p)}, \qquad d\varepsilon_{11}^{(p)} \neq 0, \tag{A.11}$$

where the plastic incompressibility has been employed. Substituting Eqs. (A.11) into Eq. (A.6) gives

$$d\varepsilon_{11}^{(p)} = \sqrt{2}d\varepsilon_0^{(p)}, \tag{A.12}$$

while substituting Eq. (A.10) into Eq. (A.2) and then into Eq. (A.7) reads

$$\tau_0 = \tfrac{\sqrt{2}}{3}\sigma_{11}. \tag{A.13}$$

Suppose that the tensile stress–strain curve of the material is composed of piecewise linear segments. Due to the well-known property in unloading process, the relationship between the plastic shear strain increment and the tensile stress increment can be denoted by

$$d\varepsilon_0^{(p)} = \frac{d\varepsilon_{11}^{(p)}}{\sqrt{2}} = \frac{1}{\sqrt{2}}\left(\frac{1}{E_T} - \frac{1}{E_{11}}\right)d\sigma.$$

Since $E_T = d\sigma/d\varepsilon_{11}$, we get

$$d\tau_0 = \frac{2M_T}{3}d\varepsilon_0^{(p)}. \tag{A.14}$$

On the other hand, differentiating Eq. (A.7) gives

$$d\tau_0 = \frac{\sigma'_{ij}}{3\tau_0}d\sigma'_{ij}.$$

Substituting Eq. (A.14) into the last equation, we obtain

$$\mathrm{d}\varepsilon_0^{(\mathrm{p})} = \frac{\sigma'_{ij}}{2M_{\mathrm{T}}\tau_0}\mathrm{d}\sigma'_{ij}. \tag{A.15}$$

From Eqs. (A.15) and (A.9), we derive

$$\mathrm{d}\varepsilon_{ij}^{(\mathrm{p})} = \frac{\sigma'_{kl}\,\mathrm{d}\sigma'_{kl}}{2M_{\mathrm{T}}\tau_0^2}\sigma'_{ij}. \tag{A.16}$$

If we make use of the assumption that no plastic work can be done by the hydrostatic component of applied stress field, i.e.

$$\sigma'_{ij}\mathrm{d}\sigma'_{ij} = \sigma'_{ij}\left(\mathrm{d}\sigma'_{ij} - \tfrac{1}{3}\mathrm{d}\sigma_{kk}\delta_{ij}\right) = \sigma'_{ij}\mathrm{d}\sigma_{ij}.$$

Eq. (A.16) can be rewritten as

$$\mathrm{d}\varepsilon_{ij}^{(\mathrm{p})} = \frac{\sigma'_{kl}\sigma'_{ij}}{2M_{\mathrm{T}}\tau_0^2}\mathrm{d}\sigma_{kl},$$

or, in the contracted form,

$$\{\mathrm{d}\varepsilon_i^{(\mathrm{p})}\} = [S_{ij}]^{(\mathrm{p})}\{\mathrm{d}\sigma_j\}. \tag{A.17}$$

where $[S_{ij}]^{(\mathrm{p})}$ is given by Eq. (6a). Substituting Eqs. (A.5) and (A.17) into Eq. (A.4), we see that the instantaneous compliance matrix has the form of Eq. (2).

References

Aboudi, J., 1984. Effective behavior of inelastic fiber-reinforced composites. Int. J. Engng. Sci. 22, 439–449.

Aboudi, J., 1988. Micromechanical analysis of the strength of unidirectional fiber composites. Comp. Sci. Technol. 33, 79–96.

Aboudi, J., 1989. Micromechanical analysis of composites by the method of cells. Appl. Mech. Rev. 42, 193–221.

Adams, D.F., 1974. Elastoplastic behavior of composites. In: Sendeckyj, G.P. (Ed.), Mechanics of Composite Materials. Academic Press, New York, pp. 169–208.

Awerbuch, J., Hahn, H.T., 1981. Off-axis fatigue of graphite/epoxy composite. ASTM STP 723, 243–273.

Beaumont, P.W.R., Schultz, J.M., 1990. Micromechanisms of fracture in continuous fiber composites – Part I: theory, failure analysis of composite materials. In: Beaumont, P.W.R., Schultz, J.M., Friedrich, K. (Eds.), Delaware Composites Design Encyclopedia, vol. 4. Technomic Publishing, Lancaster, Basel.

Chamis, C.C., 1989. Mechanics of composite materials: past, present, and future. J. Comp. Technol. Res. ASTM 11, 3–14.

Christensen, R.M., 1997. Stress based yield/failure criteria for fiber composites. Int. J. Solids Struct. 34, 529–543.

Curtin, W.A., 1993. Ultimate strengths of fiber-reinforced ceramics and metals. Composites 24, 98–102.

Echaabi, J., Trochu, F., Gauvin, R., 1996. Review of failure criteria of fibrous composite materials. Poly. Comp. 17, 786–798.

Foster, G.C., Ibnabdeljalil, M., Curtin, W.A., 1998. Tensile strength of titanium matrix composites: direct numerical simulations and analytic models. Int. J. Solids Struct. 35, 2523–2536.

Gibson, R.F. (Ed.), 1994. Principles of Composite Material Mechanics. McGraw-Hill, New York, pp. 201–207.

Gotsis, P.K., Chamis, C.C., Minnetyan, L., 1998. Prediction of composite laminate fracture: micromechanics and progressive fracture. Comp. Sci. Technol. 58, 1137–1149.

Gundel, D.B., Wawner, F.E., 1997. Experimental and theoretical assessment of the longitudinal tensile strength of unidirectional SiC-fiber/titanium–matrix composites. Comp. Sci. Tech. 57, 471–481.

Hashin, Z., Rotem, A., 1973. A fatigue failure criterion for fiber reinforced composites. J. Comp. Mater. 7, 448–464.

Hinton, M.J., Soden, P.D., 1998. Predicting failure in composite laminates: the background to the exercise. Comp. Sci. Technol. 58, 1001–1010.

Huang Zheng-ming, 2000. A bridging model prediction of the ultimate strength of composite laminates subjected to biaxial loads. Composites Sci. Technol., accepted for publication.

Hyer, M.W. (Ed.), 1997. Stress Analysis of Fiber-Reinforced Composite Materials. WCB, McGraw-Hill, Boston, pp. 120–124.

Kriz, R.D., Stinchcomb, W.W., 1979. Exp. Mech. 19, 41.

Labossiere, P., Neal, K.W., 1987. Macroscopic failure criteria for fiber-reinforced composite materials. Solid Mech. Arch. 12, 439–450.

McCullough, R.L., 1990. Micro-models for composite materials-continuous fiber composites. In: Whitney, J.M., McCullough, R.L. (Eds.), Micromechanical Materials Modeling, Delaware Composites Design Encyclopedia, vol. 2. Technomic Publishing, Lancaster.

Nahas, M.N., 1986. Survey of failure and post-failure theories of laminated fiber-reinforced composites. J. Comp. Tech. Res. 8, 138–153.

Pindera, M.J., Herakovich, C.T., 1981. An Endochronic Theory for Transversely Isotropic Fibrous Composites. VPI-E-81-27, Virginia Polytechnic Institute and State University.

Pindera, M.J., Gurdal, Z., Hidde, J.S., Herakovich, C.T., 1986. Mechanical and Thermal Characterization of Unidirectional Aramid/Epoxy, CCMS-86-08. VPI-86-29, Virginia Polytechnic Institute and State University.

Pindera, M.J., 1993. Micromechanical aspects of yielding and failure criteria of composites. In: Boehler, J.P. (Ed.), Failure Criteria of Structured Media. Balkema, Rotterdam, Netherlands, pp. 121–141.

Rowlands, R.E., 1985. Strength (failure) theories and their experimental correlation. In: Sih, G.C., Skudra, A.M. (Eds.), Failure Mechanics of Composites. North-Holland, Amsterdam, pp. 71–125.

Skudra, A.M., 1985. Micromechanics of failure of reinforced plastics. In: Sih, G.C., Skudra, A.M. (Eds.), Failure Mechanics of Composites. North-Holland, Amsterdam, pp. 1–69.

Soden, P.D., Hinton, M.J., Kaddour, A.S., 1998a. A comparison of the predictive capabilities of current failure theories for composite laminates. Comp. Sci. Tech. 58, 1225–1254.

Soden, P.D., Hinton, M.J., Kaddour, A.S., 1998b. Lamina properties, lay-up configurations and loading conditions for a range of fiber-reinforced composite laminates. Comp. Sci. Tech. 58, 1011–1022.

Soden, P.D., Kitching, R., Tse, P.C., Tsavalas, Y., Hinton, M.J., 1993. Influence of winding angle of the strength and deformation of filament-wound composite tubes subjected to uniaxial and biaxial loads. Comp. Sci. Technol. 46, 363–378.

Subramanian, S., Reifsnider, K.L., Stinchcomb, W.W., 1995. Tensile strength of unidirectional composites: the role of efficiency and strength of fiber–matrix interface. J. Comp. Tech. Res. 17, 289–300.

Teply, J.L., Reddy, J.N., 1990. Unified formulation of micromechanics models of fiber-reinforced composites. In: Dvorak, G.J. (Ed.), Inelastic Deformation of Composite Materials. Springer, New York, pp. 341–370.

Tsai, S.W., Wu, E.M., 1972. A General Theory of Strength for Anisotropic Materials, Technical Report AFML-TR-71-12, Air Force Materials Laboratory, Wright-Patterson Air Force Base, Ohio.

Tsai, S.W., Hahn, H.T., 1980. Introduction to Composite Materials. Technomic Publishing, Lancaster, Basel.